

Spray Deposition and Characterization of Nanocrystalline $\text{Cd}_{1-x}\text{Zn}_x\text{S}$ thin films

P M Parameshwari and Gopalakrishna Naik K*

*Department of Physics, Mangalore University,
Mangalagangothri - 574199, India*

Abstract

Nanocrystalline $\text{Cd}_{1-x}\text{Zn}_x\text{S}$ thin films with different zinc composition were deposited by spray pyrolysis. The influence of Zn content on the structural properties of $\text{Cd}_{1-x}\text{Zn}_x\text{S}$ was studied from the XRD spectra. The band gap of the $\text{Cd}_{1-x}\text{Zn}_x\text{S}$ thin films, which depends on the Zn composition in the solution, was determined from the absorption spectra. Transmittance of the films increases with the incorporation of Zn atoms. Blue shift in the PL peaks with the increase of Zn content in the films gives support to the formation of $\text{Cd}_{1-x}\text{Zn}_x\text{S}$ solid-solution. The electrical resistivity measurement shows that the resistivity of $\text{Cd}_{1-x}\text{Zn}_x\text{S}$ thin films increases with increase in Zn content in the film. The optical and electrical properties of the grown films are found to be suitable for solar cell applications.

Keywords: II-VI chalcogenide semiconductors, $\text{Cd}_{1-x}\text{Zn}_x\text{S}$ ternary alloy, spray pyrolysis, resistivity.

INTRODUCTION

The wide bandgap cadmium zinc sulphide ($\text{Cd}_{1-x}\text{Zn}_x\text{S}$) thin films have been under consideration for the replacement of the widely used CdS thin film window material in heterojunction solar cells¹. The relatively small bandgap (2.42 eV) of CdS window material causes a considerable solar energy absorption in the shorter wavelength region (below 500 nm) and which causes a decrease in the current density in the solar

cells¹. $\text{Cd}_{1-x}\text{Zn}_x\text{S}$ energy gap can be varied between those of CdS (2.42 eV) and ZnS (3.66 eV)², which makes it more attractive for solar cell window layers. The use of $\text{Cd}_{1-x}\text{Zn}_x\text{S}$ as window layers in heterojunction solar cells instead of CdS has led to a decrease in window absorption losses and, hence, an increase in photo current in solar cells². $\text{Cd}_{1-x}\text{Zn}_x\text{S}$ was also find applications in the fabrication of p-n junction devices without lattice mismatch with quaternary semiconductors such as CuInGaSe_2 and $\text{CuIn}(\text{S}_x\text{Se}_{1-x})_2$ ². However, the resistivity of the $\text{Cd}_{1-x}\text{Zn}_x\text{S}$ increases with increase of zinc content³. This limits their application as window layer in solar cells because the high resistivity of window layer results in an increase in the sheet resistance of p-n junction devices. To avoid the high resistivity, $\text{Cd}_{1-x}\text{Zn}_x\text{S}$ thin film with low zinc content has been under consideration as solar cell window materials. The incorporation of suitable donor impurities such as In was employed to reduce the $\text{Cd}_{1-x}\text{Zn}_x\text{S}$ thin film resistivity. Lee et. al.^{3, 4} adopted this technique in order to decrease the resistivity of chemically deposited $\text{Cd}_{1-x}\text{Zn}_x\text{S}$ by In doping. They deposited a thin layer of In on chemically deposited $\text{Cd}_{1-x}\text{Zn}_x\text{S}$ thin film by thermal evaporation, followed by heat treatment to diffuse In atoms in to the $\text{Cd}_{1-x}\text{Zn}_x\text{S}$ thin film and succeeded in decreasing the resistivity of $\text{Cd}_{1-x}\text{Zn}_x\text{S}$ up to 0.3 ohm-cm.

There have been a number of reports on the deposition of $\text{Cd}_{1-x}\text{Zn}_x\text{S}$ thin films with a range of Zn concentration using different methods like chemical bath deposition⁵, spray pyrolysis⁶, SILAR⁷, vacuum evaporation², metal organic chemical vapour deposition⁸, dip coating technique⁹ etc. In the present study nanocrystalline $\text{Cd}_{1-x}\text{Zn}_x\text{S}$ thin films were deposited by spray pyrolysis with x value ranging from 0.0 to 1.0. In this study, $\text{Cd}_{1-x}\text{Zn}_x\text{S}$ thin films were grown by varying the zinc content from x=0 to x=1 with the molar ratio of (Cd+Zn)/S fixed at 0.5. The study is mainly focused on the investigation of effects of Zn concentration on the structural, optical and electrical properties of as deposited $\text{Cd}_{1-x}\text{Zn}_x\text{S}$ thin films. The deposited films were found to have favourable optical and electrical properties for their application as a window layer in solar cells.

EXPERIMENTAL DETAILS

Nanocrystalline $\text{Cd}_{1-x}\text{Zn}_x\text{S}$ thin films were deposited on glass substrates by spray pyrolysis. Aqueous solutions of 0.15M CdCl_2 , 0.15M ZnCl_2 , and 0.15M $(\text{NH}_2)_2\text{CS}$ were used as sources of cadmium, zinc and sulphur, respectively. These precursor solutions were mixed in appropriate quantities in order to get the required composition of $\text{Cd}_{1-x}\text{Zn}_x\text{S}$, with x value 0.0, 0.2, 0.4, 0.6, 0.8 and 1.0, and stirred well for half an hour using a magnetic stirrer. In all the cases (Cd+Zn)/S molar ratio was fixed as 0.5 in order to get films with comparatively low resistivity. The films were obtained by spraying these solutions on the glass substrates kept at temperature of 400 °C at a spray rate of 10 ml per minute at an ambient atmosphere. The grown films

were allowed to cool naturally to a room temperature. The structural properties of the films were investigated by X-ray powder diffractometer (Rigaku miniflex 600) using $\text{Cu K}\alpha$ radiation ($\lambda = 1.54178 \text{ \AA}$). Full width at half maximum (FWHM) and 2θ values of the peaks was used to calculate the crystallite size. Surface morphology of these films was studied using FESEM (Hitachi SU6600). Chemical composition in the films was obtained by energy dispersive X-ray spectroscopy (EDS). Thickness of the films was measured by an Ellipsometer (Holmarc opto mechatronics, model no: HO-TCE-01) using DPSS laser (532 nm) beam. Optical properties were investigated from UV-Vis (Shimadzu 1800) absorption, transmittance and Photoluminescence (LabRAM HR Raman and MicroPL system) spectra of the films. Resistivity of the films was measured by van der Pauw method using computer controlled Keithley 236 source measure unit.

RESULTS AND DISCUSSION

Structural studies

The crystallographic properties of spray deposited nanocrystalline $\text{Cd}_{1-x}\text{Zn}_x\text{S}$ thin films have been investigated by X-ray diffraction techniques using $\text{CuK}\alpha$ radiation. The XRD spectrum was recorded in the 2θ angle ranging from $20^\circ - 60^\circ$ using Rigaku miniflex 600 X-ray diffractometer and are as shown in the Fig 1. Comparison of the prominent peak with the JCPDS data (No: 00-041-1049, 00-049-1302, 00-040-0836) shows that $\text{Cd}_{1-x}\text{Zn}_x\text{S}$ films with composition $x = 0.0, 0.2,$ and 0.4 have hexagonal crystal structure with the prominent X-ray diffraction peaks corresponding to reflections from (100), (002), (101), (102), (110), (103), (112) crystal planes. The film with composition $x = 0.6$ shows tetragonal crystal structure (JCPDS No: 01-083-2263) with prominent peak corresponding to (112) reflection and at Zn content $x = 0.8$ the structure transforms from hexagonal to cubic with dominant (111) peak (JCPDS No: 01-079-6259). The XRD pattern of ZnS is closure to amorphous structure. The XRD peak gets shifted towards the higher diffraction angle as the Zn composition increases gradually from 0.0 to 1.0 as can be seen in the Fig 1. This consecutive shift of the XRD peak indicates that the films obtained were not a mixture of CdS and ZnS, but it is a $\text{Cd}_{1-x}\text{Zn}_x\text{S}$ solid solution^{9, 10}. It is also observed that the intensity of the prominent peak gets decreased with increase of zinc content in the films, suggesting the composition dependent nature of crystallites in the films¹¹. The lattice parameter corresponding to hexagonal $\text{Cd}_{1-x}\text{Zn}_x\text{S}$ films found to be decrease with increase in the zinc composition. This is due to smaller size of the zinc atom as compared to the cadmium atom⁹.

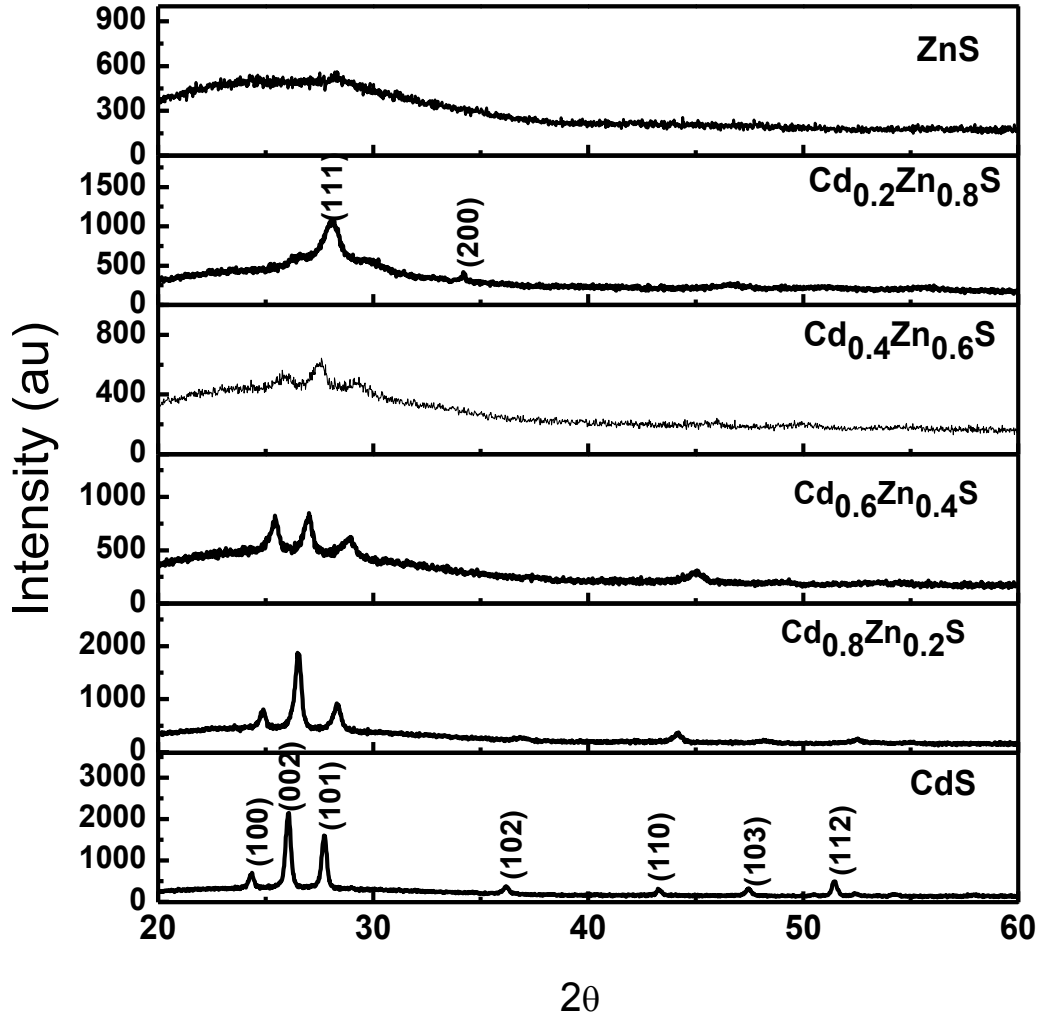


Figure 1. XRD patterns of nanocrystalline $\text{Cd}_{1-x}\text{Zn}_x\text{S}$ thin films.

The crystallite size of the films was calculated using the angle and FWHM of the prominent peak by applying Scherer's formula ¹².

$$D = \frac{k\lambda}{\beta \cos \theta} \quad (1)$$

where D is the crystallite size, k is the Scherer's constant and is equal to 0.9 for spherical crystals (wurtzite/cubic), β is the full width at half maximum (FWHM) in radians and λ is the wavelength of the x-rays (1.5406\AA for Cu- $K\alpha$). The crystallite size was found to be in the range 4 nm - 30 nm which indicates that the films are composed of nanocrystallites/nanoparticles. The crystallite size decreases with increase in zinc content in the film as illustrated in the Table 1.

Table 1: Crystallite size, and strain in the $Cd_{1-x}Zn_xS$ thin films

Zn content in solution (x)	Crystallite size (nm)	Strain $\times 10^{-3}$
0.0	30.07	5.11
0.2	23.69	6.37
0.4	18.39	8.07
0.6	9.66	14.5
0.8	4.17	34.1

Strain developed in the films was calculated from FWHM of prominent peaks using the relation¹²

$$\varepsilon = \beta \cot \theta / 4 \quad (2)$$

The strain in the film increases with increase in the zinc percentage in the film and is in the order of 10^{-3} which is listed in the Table 1. Inverse relation between the crystallite size and the strain developed in the films was clearly observed from these results.

Surface morphology and elemental composition analysis

FESEM image of spray deposited nanocrystalline $Cd_{1-x}Zn_xS$ thin films with x value ranging from 0.0 to 1.0 are as shown in the Figure 2(a-f). The significant influence of Zn content on the surface morphology can be clearly identified from these images. The growth of the films was found to be uniform, dense and well adherent to the substrate surface. The surface smoothness of the films was found to be increase with gradual increase of zinc content from 0.0 to 1.0. Elemental composition in the films was examined from the EDS. The zinc content in the films was found to be increase with increase in zinc amount in the spray solution and compositions in the films are indistinguishable from that in the initial solution. This indicates that there is no loss of elements during the spray deposition process. The comparison of elemental composition in the solution and that in the deposited films are given in the Table 2.

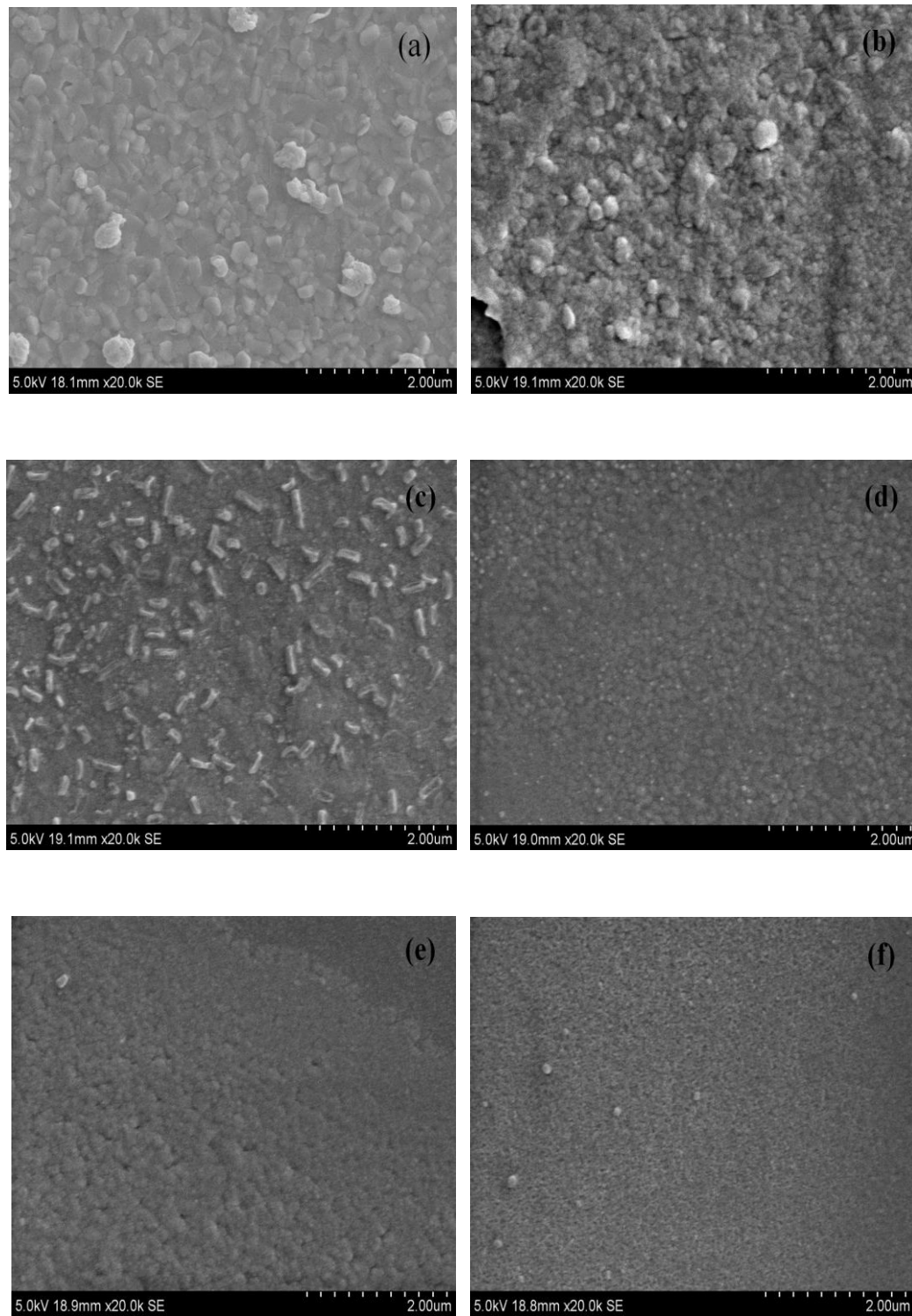


Figure 2. FESEM images of $\text{Cd}_{1-x}\text{Zn}_x\text{S}$ thin films with (a) $x = 0.0$ (b) $x = 0.2$ (c) $x = 0.4$ (d) $x = 0.6$ (e) $x = 0.8$ and (f) $x = 1.0$.

Table 2: Elemental composition in the $Cd_{1-x}Zn_xS$ thin films

Composition , x in solution	Cadmium (%)	Zinc (%)	Sulphur (%)	Composition , x in film
0.0	49.71	-	50.28	0.0
0.2	43.83	7.00	49.16	0.14
0.4	27.63	17.17	55.20	0.38
0.6	23.08	27.88	49.05	0.55
0.8	11.24	39.97	48.97	0.78
1.0	-	50.19	49.81	1.0

Optical studies

The optical absorption spectra of the nanocrystalline $Cd_{1-x}Zn_xS$ thin films were recorded in the wavelength range 300 nm – 800 nm using Shimadzu 1800 spectrophotometer. The fundamental absorption edge shows a blue shift with an increase in the zinc ion content in the film as can be seen in the Figure 3(a). Thickness of the films was measured using a Holmarc Opto-Mechatronics single wavelength ellipsometer. The ellipsometer consists of a laser (532 nm, randomly polarized), a polarizer (Glan-Thompson Prism) and a quarter wave plate which provide a state of polarization which can be varied from linearly polarized light to elliptically polarized light to circularly polarized light by varying the angle of the polarizer. For the measurement of the thin film thickness, the polarized laser beam is made to incident on the thin film sample at an angle of incidence 70° . The reflected beam is analyzed with the analyzer (Glan-Thompson Prism) and the detector. The angles of the polarizer and analyzer were changed until a minimal signal (or null condition) is detected. The corresponding angles of the polarizer and analyzer were measured. Software provided along with the instrument is used to calculate the thickness of the films. All the films have ~190 nm in thickness. From the thickness of the film d , optical absorbance A , the absorption coefficient (α) can be calculated using the Lambert law¹³

$$\ln \frac{I}{I_0} = 2.303 A = \alpha d \quad (3)$$

where I_0 and I are the intensity of incident and transmitted light respectively. The band gap E_g of the semiconductor films can be obtained using the Tauc relation¹² for an optical absorbance,

$$\alpha h\nu = B(h\nu - E_g)^n \quad (4)$$

where B is a constant, $h\nu$ is the energy of light and the exponent 'n' characterizes the nature of band transition, $n = 1/2$ for direct band gap semiconductor material. The graph of $h\nu$ versus $(\alpha h\nu)^2$ are plotted as shown in the Figure 3(b). The linear nature of the graph at the absorption edge confirmed that as deposited films are direct band gap semiconductor⁵. The extrapolation of straight line portion of the curve to the energy axis gives the band gap values and these are listed in the Table 3.

Table 3: Energy gap and resistivity variation with zinc content in the $\text{Cd}_{1-x}\text{Zn}_x\text{S}$ thin film.

Composition x in solution	Energy gap (eV) from Uv-vis absorption spectra	Resistivity (ohm-cm)
0.0	2.466	3.32×10^2
0.2	2.613	2.26×10^3
0.4	2.817	8.23×10^3
0.6	3.00	4.87×10^4
0.8	3.246	6.75×10^4
1.0	3.636	2.80×10^4

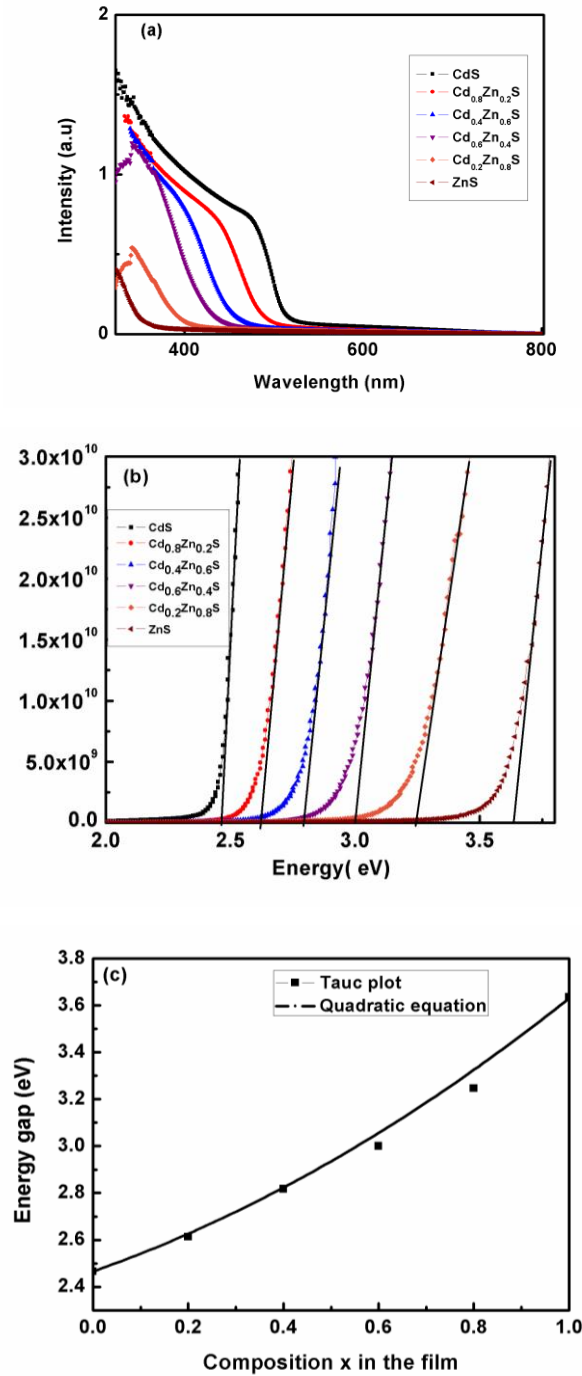
This band gap values determined from optical absorption spectroscopy varies almost linearly with composition between that of CdS (2.466 eV) and ZnS (3.636 eV). This linear relationship between the band gap and composition in the films again confirms the formation $\text{Cd}_{1-x}\text{Zn}_x\text{S}$ thin films⁹.

The band gap of $\text{Cd}_{1-x}\text{Zn}_x\text{S}$ thin films was calculated in range x from 0 to 1 using the quadratic relation

$$E_g (\text{Cd}_{1-x}\text{Zn}_x\text{S}) = x E_g \text{ZnS} + (1-x) E_g \text{CdS} - bx(1-x) \quad (5)$$

where b is the bowing parameter⁶. The value of b was obtained by fitting Eq. (5) with the experimental data using the experimentally obtained values of $E_{g\text{CdS}}$ (2.466 eV) and $E_{g\text{ZnS}}$ (3.636 eV) and it was found to be 0.45. The variation in band gap of the $\text{Cd}_{1-x}\text{Zn}_x\text{S}$ thin films with Zn content, obtained from absorbance spectra and that calculated using Eq. (5) is shown in Figure 3(c). The optical transmittance spectra of the films were recorded in the wavelength range 300 nm – 1000 nm. Transmittance of the films increases with increase in zinc content as plotted in the Figure 3(d). Transmittance spectra also show a sharp fall at the absorption edge, which is an

indication of the good crystallinity of the films¹. The increase in transmittance with increase in zinc content was also reported by many groups¹⁰. Relatively high transmission above fundamental absorption edge reveals that the films are weakly absorbing in the wavelength range above the band edge to 1000 nm.\



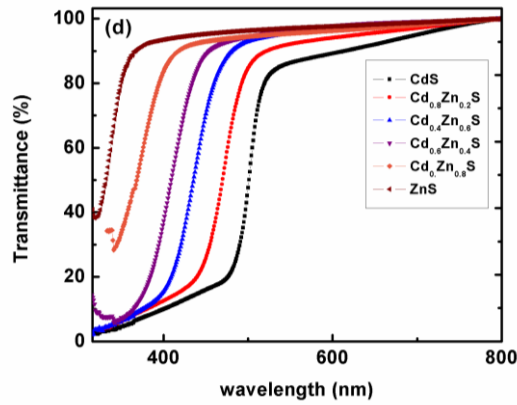
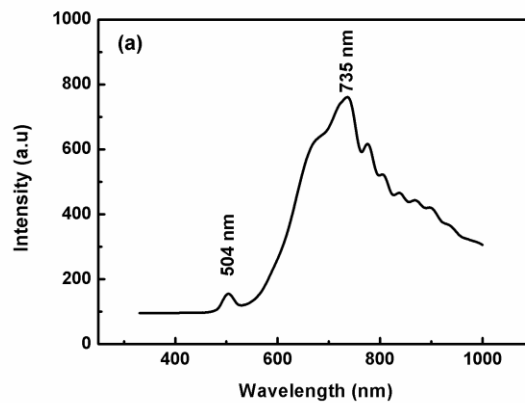


Figure 3. (a) UV-Vis absorption spectra (b) $h\nu$ vs. $(\alpha h\nu)^2$ plot (c) Variation in energy gap and (d) Transmittance spectra, of $\text{Cd}_{1-x}\text{Zn}_x\text{S}$ thin films.

The room temperature PL spectra of nanocrystalline $\text{Cd}_{1-x}\text{Zn}_x\text{S}$ thin films are as shown in the Figure 4(a – f). PL spectrum of CdS thin film shows peaks at 504 nm and 734 nm. The green emission band at around 504 nm can be attributed to interstitial sulphur and the peak at 704 nm is related to the sulphur vacancy¹⁴. From Figure 4(b – f), it was observed that the emission peaks of $\text{Cd}_{1-x}\text{Zn}_x\text{S}$ thin films shifts from 654 nm to 524 nm as x value increases from 0.2 to 1.0. This blue shift in the emission spectra gives evidence to the formation of $\text{Cd}_{1-x}\text{Zn}_x\text{S}$ solid solution¹⁰. In all the films the emission peak is observed at wavelength higher than corresponding band gap wavelengths of the films. This indicates that the radiative transition occurred from defect states rather than excitonic transition¹⁵. It is also observed that the intensity of PL peaks decreases with increase of Zn content in the films. This quenching effect in PL spectra may be attributed to the changes in the structural properties of the film by the incorporation of Zn atoms. A similar PL quenching effect due to structural changes in In doped CdS was reported by Abdolazadeh Ziabari A and Ghodsi F.E¹⁶.



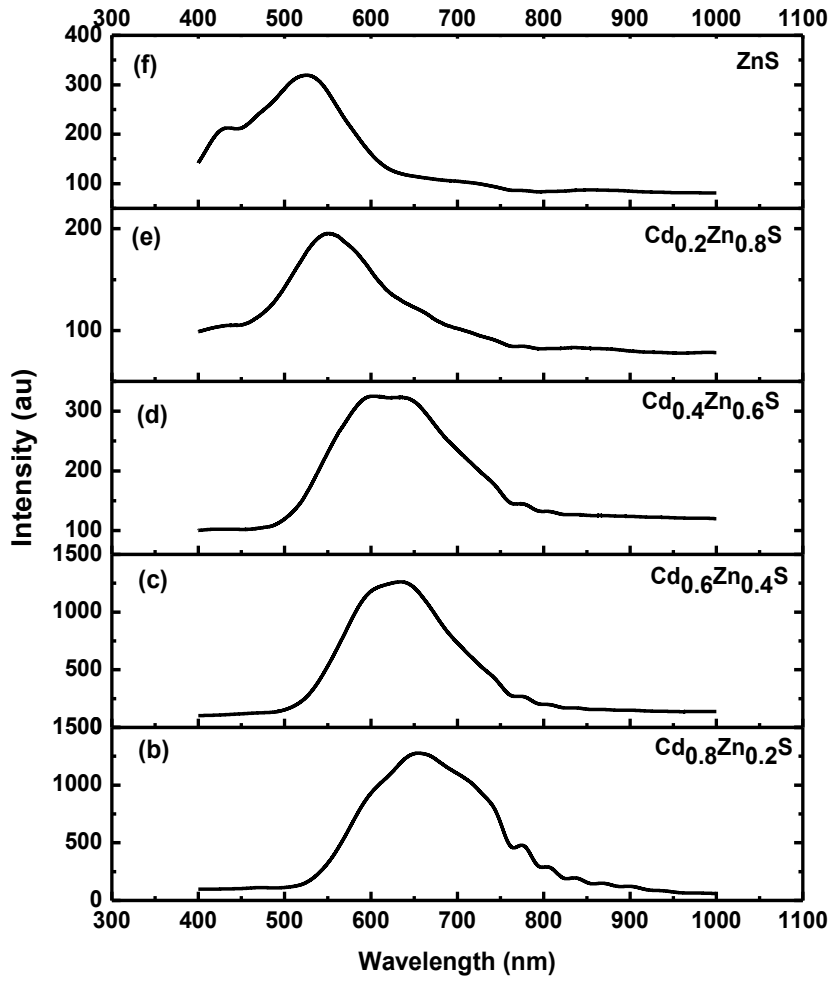


Figure 4. Room temperature PL spectra of (a) CdS (b) $\text{Cd}_{0.8}\text{Zn}_{0.2}\text{S}$ (c) $\text{Cd}_{0.6}\text{Zn}_{0.4}\text{S}$ (d) $\text{Cd}_{0.4}\text{Zn}_{0.6}\text{S}$ (e) $\text{Cd}_{0.2}\text{Zn}_{0.8}\text{S}$ (f) ZnS thin films.

Electrical properties

The linear current voltage (I-V) characteristics shown in Figure 5 indicate the Ohmic nature of the electrical contacts. Room temperature resistivity's ρ of as deposited $\text{Cd}_{1-x}\text{Zn}_x\text{S}$ ($0 \leq x \leq 1$) thin films were measured by van der Pauw method using PC controlled Keithley 236 source measure unit. The resistivity of $\text{Cd}_{1-x}\text{Zn}_x\text{S}$ increases from 3.32×10^2 ohm-cm to 6.75×10^4 ohm-cm with increase of Zn content in the film from 0.0 to 0.8, which is shown in Table 3. This increase in resistivity with increase of Zn composition can be attributed to decrease in grain size, thus increase of number of grain boundaries, and also increase of the grain boundary scattering due to

charges¹⁷. The resistivity values obtained in this study are too smaller compared to that reported by Lee et. al.² for $\text{Cd}_{1-x}\text{Zn}_x\text{S}$ thin films deposited by co-evaporation of ZnS and CdS, they obtained a resistivity of 2.7×10^7 ohm-cm for $\text{Cd}_{1-x}\text{Zn}_x\text{S}$ thin films with $x = 0.35$. Cruz et.al.¹⁸ reported a resistivity of 9.7 ohm-cm for chemical bath deposited CdS thin films by Zn (1 at%) doping. Literature survey shows that the films having this range of resistivity are suitable for the photovoltaic device applications¹⁹. For further decrease of resistivity of $\text{Cd}_{1-x}\text{Zn}_x\text{S}$ thin films indium doping before / after the deposition is useful^{3,4}.

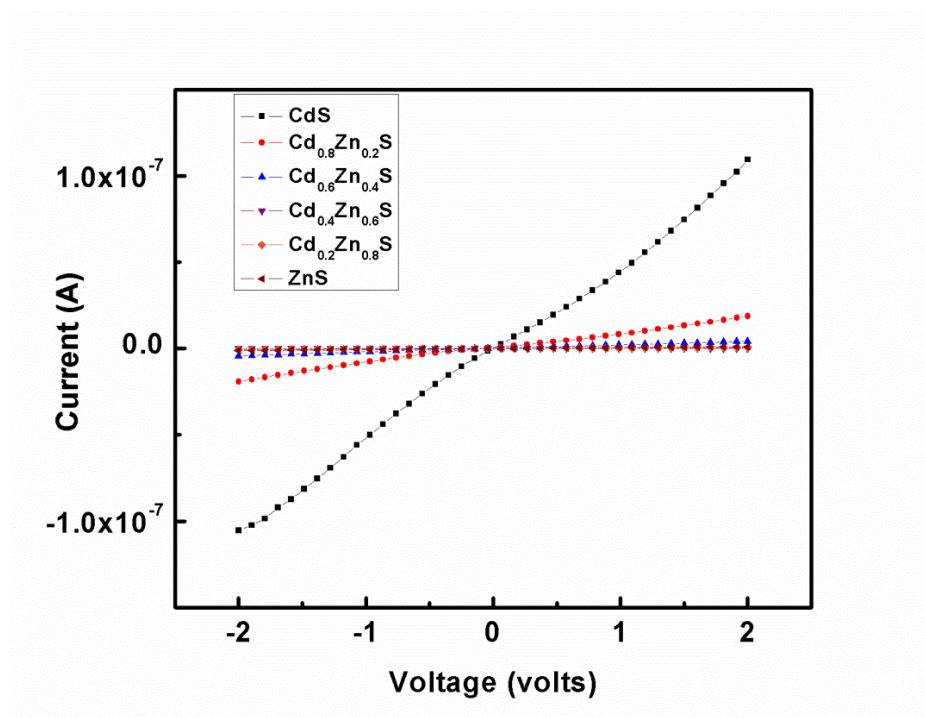


Figure 5. Current – Voltage characteristics of $\text{Cd}_{1-x}\text{Zn}_x\text{S}$ thin films

CONCLUSIONS

Nanocrystalline $\text{Cd}_{1-x}\text{Zn}_x\text{S}$ thin films were successfully deposited using an aqueous solutions of CdCl_2 , ZnCl_2 and $(\text{NH}_2)_2\text{CS}$ by spray pyrolysis. Analysis of XRD spectra reveals the nanocrystalline nature of the films. Influence of Zn content on the surface morphology of the films was confirmed from FESEM and EDX studies. The fundamental absorption edge of the as-deposited $\text{Cd}_{1-x}\text{Zn}_x\text{S}$ thin films showed a blue shift with an increase in the zinc ion content. Transmittance of the films increased with increase of zinc content in the film. Intensity of PL emission peaks decreased and blue shifted with the increase of Zn content in the films. The transmittance and the resistivity values of the films deposited in this study are suitable for their

application as a window layer in the thin film heterojunction solar cells with CdTe, CIGS, and CuInS₂ as an absorber layer.

ACKNOWLEDGEMENTS

The authors are grateful to the DST-PURSE Project (MU/CHEM/PURSE PIG/2012) of the Mangalore University and UGC, Govt. of India for providing financial support (RFSMS). The authors acknowledge INUP, Center for Nanoscience, IISc, Bangalore for providing characterization facility. The authors acknowledge Abdul Rasheed P, School of Nanoscience and Technology, National Institute of Technology, Calicut for his help in FESEM – EDX characterisation.

REFERENCES

- [1] Xia, W., Welt, J. A., Lin, H., Wu, H. N., Ho, M. H. & Tang, C. W., 2010, Fabrication of Cd_{1-x}Zn_xS films with controllable zinc doping using a vapor zinc chloride treatment, *Solar Energy Materials & Cells*, 94, 2113-2118.
- [2] Lee J. H., Song, W. C., Yi, J. S., Yang, K. J., Han, W. D., Hwang, J., 2003, Growth and properties of the Cd_{1-y}Zn_yS thin films for solar cell Applications, *Thin Solid Films*, 431 –432, 349-353.
- [3] Lee J. H., Song, W. C., Yang, K. J., Yoo, Y. S., 2002, Characteristics of the CdZnS thin film doped by indium diffusion, *Thin Solid Films*, 416, 184-189.
- [4] Lee J. H., Song, W. C., Yi, J. S., Yoo, Y. S., 2003, Characteristics of the CdZnS thin film doped by thermal diffusion of vacuum evaporated indium films, *Solar Energy Materials & Solar Cells*, 75, 227-234.
- [5] Chavhan S. D., Senthilarasu S., Soo-Hyoung Lee, 2008, Annealing effect on the structural and optical properties of a Cd_{1-x}Zn_xS thin film for photovoltaic applications, *Applied Surface Science*, 254, 4539-4545.
- [6] Baykul C. M., Orhan, N., 2010, Band alignment of Cd_(1-x)Zn_xS produced by spray pyrolysis method, *Thin Solid Films*, 518, 1925-1928.
- [7] Laukaitis G., Lindroos S., Tamulevicius S., Leskela M., Rackaitis M., 2000, SILAR deposition of Cd_xZn_{1-x}S thin films, *Applied Surface Science*, 161, 396-405.
- [8] Clayton A. J., Irvine S. J. C., Jones E. W., Kartopu G., Barrioz V., Brooks W. S. M., 2012, MOCVD of Cd_(1-x)Zn_(x)S/CdTe PV cells using an ultra-thin absorber layer, *Solar Energy Materials & Solar Cells*, 101, 68-72.

- [9] Sekhar C. Ray, Malay K. Karanjai, Dhruba Das Gupta, 1998, Deposition and characterization of $\text{Cd}_{1-x}\text{Zn}_x\text{S}$ thin films prepared by the dip technique, *Thin Solid Films*, 322, 117-122.
- [10] Jana S., Maity R., Das S., Mitra M. K., Chattopadhyay K. K., 2007, Synthesis, structural and optical characterization of nanocrystalline ternary $\text{Cd}_{1-x}\text{Zn}_x\text{S}$ thin films by chemical process, *Physica E*, 3109-3114.
- [11] Xing, C., Zhang, Y., Yan, W., Guo, L., 2006, Band structure-controlled solid solution of $\text{Cd}_{1-x}\text{Zn}_x\text{S}$ photocatalyst for hydrogen production by water splitting *International Journal of Hydrogen Energy*, 31, 2018-2024.
- [12] Kumar, S., Sharma, P., and Sharma, V., 2012, CdS nanofilms: Synthesis and the role of annealing on structural and optical properties, *J. Appl. Phys.* 111, 113510.
- [13] Chu, J., Jin, Z., Cai, S., Yang, J. X., Hong, Z., 2012, *Thin Solid Films*, 520, 1826-1831.
- [14] Aguilar-Hernández, J., Sastré-Hernández, J., Mendoza-Pérez, R., Contreras-Puente, G., Cardenas-Garcia, M., Ortiz-Lopez, J., 2006, Photoluminescence studies of CdS thin films annealed in CdCl_2 atmosphere, *Solar Energy Materials & Solar Cells*, 90, 704-712.
- [15] Bhattacharjee, B., Mondal, S. K., Hakrabarti, K., Ganguli, D., Chaudhuri, S., 2002, Optical properties of $\text{Cd}_{1-x}\text{Zn}_x\text{S}$ nanocrystallites in sol-gel silica matrix, *J. Phys. D: Appl. Phys.* 35, 2636-2642.
- [16] Abdolazadeh Ziabari, A., Ghodsi, F. E., 2013, Influence of Cu doping and post-heat treatment on the microstructure, optical properties and photoluminescence features of sol-gel derived nanostructured CdS thin films, *Journal of Luminescence*, 141, 121-129.
- [17] Oztas, M., and Bedir, M., 2008, Thickness dependence of structural, electrical and optical properties of sprayed ZnO:Cu films, *Thin Solid Films*, 516, 1703-1709.
- [18] Cruz, S. J., Perez, C. R., Delgado, T. G., Angel, Z. O., 2010, CdS thin films doped with metal-organic salts using chemical bath deposition, *Thin Solid Films*, 518, 1791-1795.
- [19] Yamaguchia, T., Tanaka, Y. T. T., Yoshida, A., 1999, Preparation and characterization of (Cd,Zn)S thin films by chemical bath deposition for photovoltaic devices, *Thin Solid Films*, 343-344, 516-519.